

Regime-Switching Bayesian Digital Twins for Two-Phase Wellbore Hydraulics and Early Kick Recognition Under Partial Observability

Aarav Shrestha^a, Kiran Adhikari^b, Milan Bhattarai^c

Abstract:

Multiphase flow in wellbores and near-wellbore conduits remains a central uncertainty driver in drilling automation and managed-pressure operations, especially when the available measurements are sparse, delayed, and dominated by surface instrumentation. In practice, operators must infer downhole pressure, holdup, and evolving flow patterns from noisy standpipe pressure, choke states, pump schedules, and occasional density estimates, while simultaneously maintaining the bottom-hole pressure within narrow operational limits. This paper presents a probabilistic digital-twin framework that treats two-phase hydraulics as a stochastic hybrid dynamical system whose continuous states follow reduced-order two-fluid physics, while an unobserved discrete regime process governs closure behavior, transient mixing, and slip. The proposed model couples a regime-switching state-space formulation with Bayesian inference to provide time-resolved posterior distributions over pressure and gas fraction along the wellbore, and to produce calibrated probabilities of abnormal gas influx. The main technical contribution is an inference-and-control stack that fuses physics-consistent propagation with sequential probabilistic learning of regime-dependent closures, enabling coherent uncertainty quantification and risk-aware decisions. The approach is designed to work with heterogeneous data sources and to remain well-posed when only surface pressure is continuously available. Simulation studies across vertical and deviated segments demonstrate that regime uncertainty can be separated from influx uncertainty when the model explicitly represents closure switching and measurement delays, reducing false alarms while preserving rapid detection in low signal-to-noise scenarios.

Copyright © Morphpublishing Ltd.

1. Introduction

Reliable estimation of downhole conditions during drilling is constrained by sensing limitations and by the intrinsic complexity of gas–liquid dynamics in confined geometries [1]. Even when the fluid system is nominally described by

^a Himalayan Institute of Technology, Mandikatar Road, Kathmandu, Nepal

^b Gandaki University of Science and Technology, Lamachaur-16, Pokhara, Nepal

^c Lumbini City College, Kalikanagar Road, Butwal, Nepal

This is an open-access article published by MorphPublishing Ltd. under a Creative Commons license. MorphPublishing Ltd. is not responsible for the views and opinions expressed in this publication, which are solely those of the authors.

conservation laws, practical predictions require empirical closures for slip, friction, interfacial momentum exchange, entrainment, and transient mixing. These closures are known to change qualitatively with flow pattern and orientation, and the mapping from superficial velocities to regimes is not static when the system is accelerating, aerating, and subject to boundary perturbations induced by pumps and chokes. In parallel, the decision problem is inherently risk-driven: the cost of late recognition of an abnormal influx is high, but the cost of frequent false alarms can also be substantial when it triggers unnecessary nonproductive time and unstable control actions.

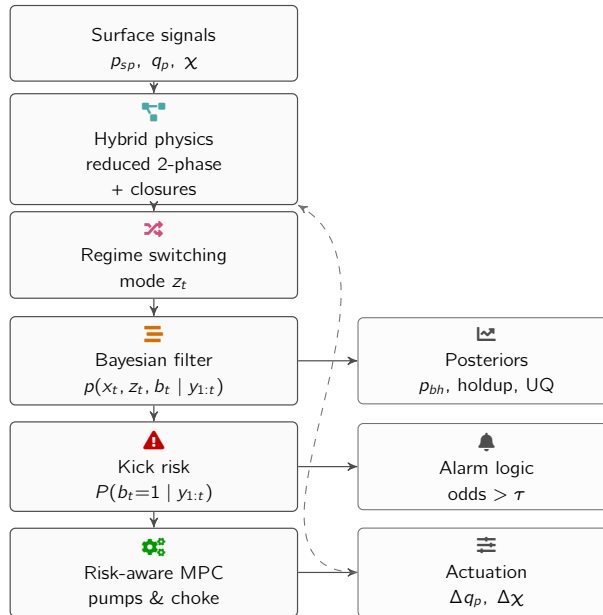


Figure 1. Online probabilistic digital-twin stack: surface measurements and control inputs feed a hybrid two-phase hydraulics model with latent regime switching, enabling Bayesian filtering for state uncertainty quantification and calibrated kick-risk probabilities that drive risk-aware control and alarm logic.

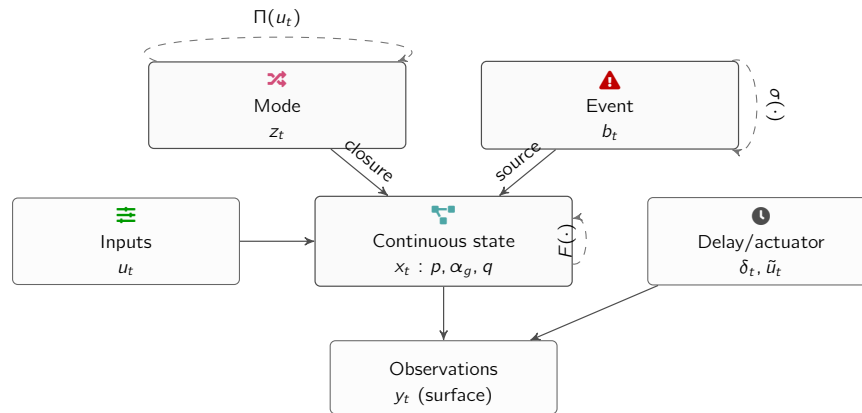


Figure 2. Hybrid state-space representation under partial observability: the continuous hydraulics state x_t is governed by regime-dependent closures (mode z_t) and a sparse abnormal-influx process (indicator b_t), while surface observations y_t are produced through delay and actuator dynamics.

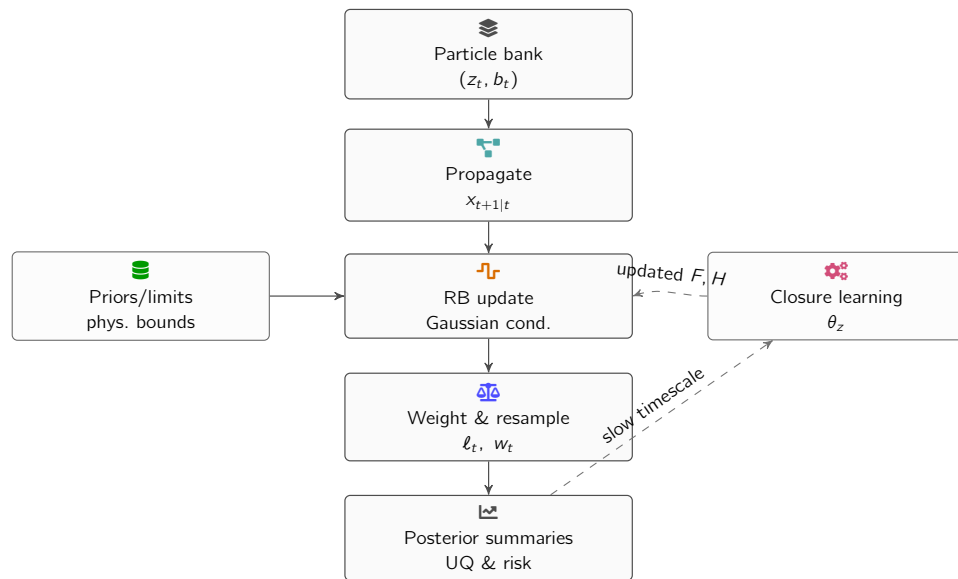


Figure 3. Rao–Blackwellized particle filtering with regularized closure learning: discrete particles track (z_t, b_t) while a conditional Gaussian update tracks continuous hydraulics, enabling stable uncertainty propagation and gradual adaptation of regime-dependent closures.

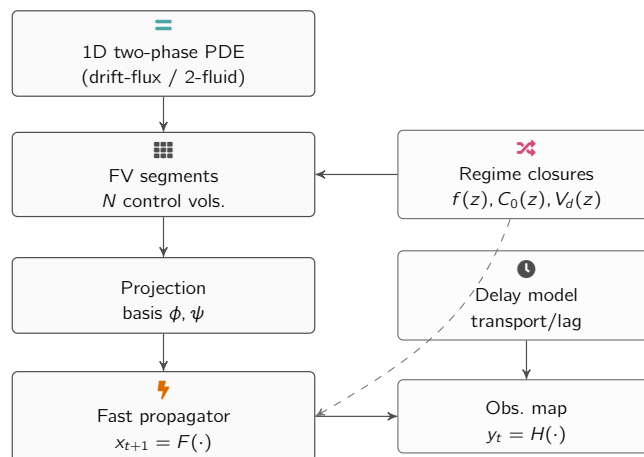


Figure 4. Reduced-order hydraulics construction for sequential inference: a quasi-1D two-phase model is discretized conservatively, then projected to a compact latent state for fast propagation, with regime-conditioned closures and an explicit delay-aware observation model linking latent downhole dynamics to surface signals.

Data-driven regime identification has demonstrated that regime labels can be extracted with high accuracy from curated experimental features when the operating envelope and geometry are known. For example, classification in vertical gas–liquid flow can approach near-deterministic performance for certain datasets when the feature space is well chosen and the models are carefully validated; a cross-validated nearest-neighbor approach was reported to achieve 98% test accuracy for vertical regime labeling over multiple distinct regions [2]. Such results are informative,

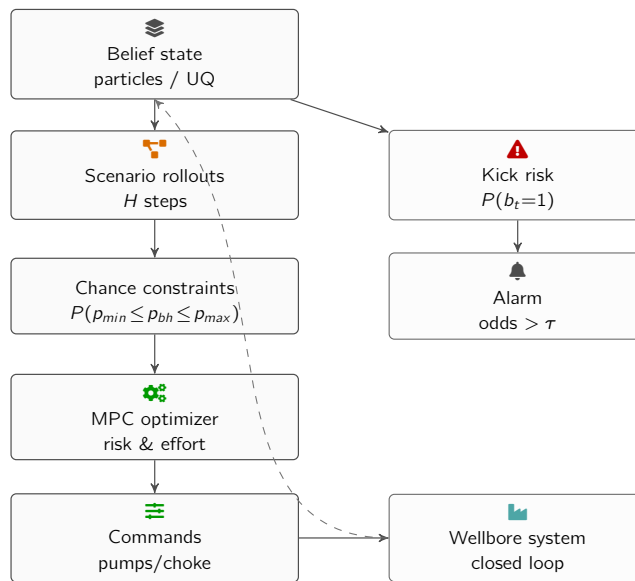


Figure 5. Risk-aware well-control integration: posterior beliefs drive scenario rollouts and chance constraints for maintaining bottom-hole pressure inside the operational window, while kick-risk probability supports graded alarms and risk-weighted control actions in closed loop.

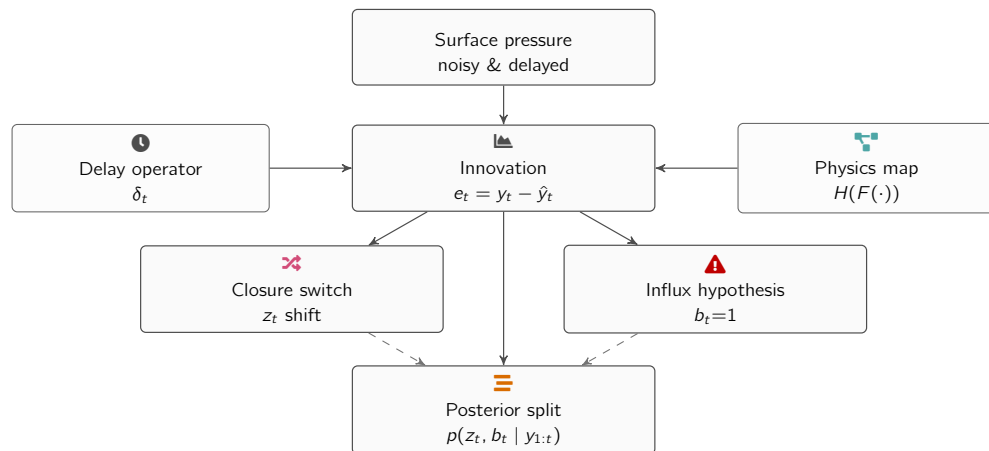


Figure 6. Separating regime uncertainty from influx uncertainty under partial observability: the innovation sequence is explained either by closure switching (mode-dependent mismatch) or by an abnormal gas source, with explicit delay modeling improving phase alignment so posterior mass can be allocated consistently between competing explanations.

yet they leave open several operational gaps. Field measurements rarely provide the same features available in flow-loop studies, temporal transitions and delays matter, and the decision objective is not merely to label a regime but to safely steer the system under uncertainty while diagnosing abnormal events such as gas influx.

The central premise of this paper is that regime identification and early kick recognition should be treated as coupled inference tasks within a single probabilistic dynamical model rather than as separate classification steps. The two-phase system is modeled as a stochastic hybrid process with continuous latent states representing pressure,

phase holdup, and mixture flow variables, and with a discrete latent mode representing regime-dependent closure structure. The discrete mode is not simply an output label; it is a causal mediator that determines how the physics propagates between measurement times [3]. Within this perspective, a regime map becomes a prior over mode occupancy conditioned on operating inputs, while transient data updates the posterior distribution over both mode and state. By explicitly modeling mode switching, the method seeks to prevent a common failure mode in purely continuous models: compensating for closure mismatch by incorrectly inferring an influx, or compensating for an influx by over-adjusting friction and slip parameters.

The technical contribution is organized around three coupled elements. The first is a reduced-order two-fluid representation that preserves the key transport and compressibility effects relevant to drilling hydraulics while remaining computationally tractable for sequential inference. The second is a regime-switching state-space model that connects the reduced-order physics to surface measurements through realistic delay and distortion operators, thereby producing a coherent likelihood for Bayesian filtering [4]. The third is an inference-and-control stack that computes calibrated posterior probabilities of abnormal influx and uses these probabilities within a risk-aware control objective that respects pressure-window constraints in a probabilistic sense. The resulting digital twin is intended to operate as an online estimator and decision support module that can ingest pump schedules and choke commands, update its beliefs in real time, and expose uncertainty measures suitable for automation.

A key design choice is to represent uncertainty at multiple levels. Parametric uncertainty captures unknown friction multipliers, slip coefficients, and interfacial exchange strengths that are specific to the configuration and can drift over time. Structural uncertainty is captured by the discrete regime process, which modifies which closure families are active and how quickly transitions occur [5]. Measurement uncertainty accounts for sensor noise, quantization, and systematic bias. Finally, unmodeled disturbances are represented as stochastic process noise whose magnitude can depend on the inferred regime, reflecting the empirical observation that certain patterns lead to stronger fluctuations and intermittency. This multi-layered uncertainty representation is essential for separating ordinary transient variability from the early signatures of abnormal influx, particularly when the available measurements are dominated by surface pressure signals and when the system is subject to active control.

The remainder of the paper develops the modeling and inference framework, derives learning rules for regime-dependent closures, and describes an evaluation protocol designed to test detection performance under realistic constraints. The emphasis is on a technical formulation that can be implemented in a digital-twin setting, rather than on proposing a new regime taxonomy [6]. The regime process is treated as an abstract mode variable that can represent any operationally meaningful partitioning of closure behavior, including but not limited to classical regime names.

2. Governing Models and Reduced-Order Representation

Table 1. Uncertainty layers in the hybrid model

Layer	Examples	Mainly affects
Parametric	f , C_0 , V_d	Pressure drop, slip
Structural	Mode z_t grid	Closure families
Measurement	Noise, bias, gaps	Likelihood R
Process	w_t intensity	State evolution $Q(z_t)$
Prior	Bounds, hyperpriors	Learning stability

Table 2. Main variable groups in the digital twin

Group	Symbols	Role
Continuous state	x_t	Reduced hydraulics and actuators
Discrete regime	z_t	Closure and pattern index
Influx indicator	b_t, r_t	Kick activity and rate
Inputs	u_t	Pump and choke commands
Config/geometry	$\theta(t)$	Depth, inclination, diameters
Observations	y_t	Surface pressure and flow signals

Table 3. Reduced-order hydraulics state contents

Field	Symbols	Representation
Pressure	p_i, η_r	Segment values or pressure modes
Gas fraction	α_i, ξ_r	Local holdup or projected basis
Mixture flux	q_i, u_m	Interface or mixture flow rate
Actuator states	\tilde{u}_t	Pump and choke dynamics
Delay states	δ_t	Transport and acoustic lags

Table 4. Regime-dependent closure elements

Closure item	Symbol	Regime effect
Distribution parameter	$C_0(\cdot, z)$	Phase split of mixture flux
Drift velocity	$V_d(\cdot, z)$	Gas-liquid relative motion
Friction factor	$f(z)$	Wall and cuttings friction level
Transient term	$S_{tr}(z)$	Intermittent momentum losses
Noise covariance	$Q(z)$	Fluctuation strength per mode

Table 5. Hybrid state-space formulation components

Component	Law	Interpretation
Mode dynamics	$z_{t+1} \sim \text{Cat}(\Pi(u_t))$	Regime switching Markov chain
State dynamics	$x_{t+1} \sim \mathcal{N}(F(\cdot), Q(z_t))$	Propagated hydraulics state
Observation	$y_t \sim \mathcal{N}(H(\cdot), R)$	Surface and equipment signals
Affine approx.	A, B, c, G	Local linearization of F
Output map	C, D, d	Linearized H around operating point

Table 6. Abnormal influx latent-process specification

Item	Symbol	Role
Event indicator	b_t	On/off state for influx
Persistence prior	κ_0, κ_1	Controls burst duration
Influx rate	r_t	Gas mass injection into annulus
Rate prior	μ_r, σ_r^2	Log-normal magnitude model
Entry location	i^*	Segment where gas enters
Risk signal	$P(b_t = 1 \mathcal{D}_t)$	Probability used for alarms

A drilling hydraulics model suitable for online inference must strike a balance between physical fidelity and computational tractability. Full three-dimensional multiphase computational fluid dynamics is not appropriate for

Table 7. Rao–Blackwellized particle filter structure

Item	Symbol	Type	Meaning
Particle index	n	Integer	Scenario label
Discrete path	$z_t^{(n)}, b_t^{(n)}$	Categorical	Mode and event history
State mean	$\mu_t^{(n)}$	Vector	Conditional estimate of x_t
State covariance	$P_t^{(n)}$	Matrix	Conditional uncertainty of x_t
Weight	$w_t^{(n)}$	Scalar	Normalized importance factor

Table 8. Risk-aware pressure control ingredients

Element	Expression	Function
Pressure window	p_{\min}, p_{\max}	Lower and upper limits
Chance constraint	$\mathbb{P}(p_{\min} \leq p_{bh} \leq p_{\max})$	Safety under uncertainty
Tracking term	$(p_{bh} - p_{ref})^2$	Follow reference trajectory
Move penalty	$\lambda \ u_t - u_{t-1}\ ^2$	Smooth pump and choke actions
Risk penalty	$\rho \mathbb{E}[\text{Risk}(b_t)]$	Bias actions under kick risk
Info gain	$-\gamma \mathcal{H}(P(b_t = 1 \cdot))$	Encourage disambiguating tests

Table 9. Key evaluation metrics for the digital twin

Metric	Symbol / notion	Focus
BH pressure error	$\text{RMSE}(p_{bh})$	Latent pressure accuracy
Surface pressure error	$\text{RMSE}(p_{\text{surf}})$	Fit to standpipe data
Calibration	Credible set coverage	Reliability of posterior bands
Sharpness	Interval width	Concentration of beliefs
Detection delay	Time to alarm	Onset speed for kicks
False alarms	Count / rate	Spurious detection frequency

Table 10. Representative scenario classes used in case studies

Scenario	Features	Main stress point
Nominal circulation	No influx, varying inclination	Baseline estimation quality
Controlled ramps	Pump and choke transients	Delay and compressibility handling
Simulated influx	Local gas entry	Regime vs influx separation
Hybrid logs	Real inputs, simulated downhole	Robustness to data artefacts
Multi-segment wells	Vertical–deviated–horizontal	Orientation and regime changes

sequential filtering under operational time constraints, while overly simplified algebraic pressure-loss models can obscure the temporal structure needed for early abnormal-event recognition. The approach adopted here begins from a one-dimensional two-fluid description along a curvilinear coordinate s that follows the wellbore centerline, with inclination $\theta(s)$ measured relative to vertical and with cross-sectional area $A(s)$ and hydraulic diameter $D_h(s)$ allowed to vary slowly in s . The phases are indexed by $k \in \{g, l\}$ for gas and liquid, with volumetric fractions $\alpha_k(s, t)$ satisfying $\alpha_g + \alpha_l = 1$, velocities $u_k(s, t)$, densities $\rho_k(p, T)$, and a common pressure $p(s, t)$ under the standard assumption of negligible radial pressure variation.

A compressible two-fluid model can be written as phase continuity and momentum equations with source terms representing interphase mass transfer, wall friction, and interfacial momentum exchange [7]. A representative form

is

$$\frac{\partial}{\partial t} (\alpha_g \rho_g) + \frac{\partial}{\partial S} (\alpha_g \rho_g u_g) = \Gamma_g, \quad (1)$$

$$\frac{\partial}{\partial t} (\alpha_l \rho_l) + \frac{\partial}{\partial S} (\alpha_l \rho_l u_l) = \Gamma_l, \quad (2)$$

$$\frac{\partial}{\partial t} (\alpha_k \rho_k u_k) + \frac{\partial}{\partial S} (\alpha_k \rho_k u_k^2) = -\alpha_k \frac{\partial p}{\partial S} - \alpha_k \rho_k g \cos \theta + \mathcal{F}_{w,k} + \mathcal{F}_{i,k} + u_k \Gamma_k, \quad (3)$$

where g is gravitational acceleration, Γ_k are mass source terms, $\mathcal{F}_{w,k}$ are wall friction forces per unit volume, and $\mathcal{F}_{i,k}$ are interfacial momentum exchange terms that satisfy $\mathcal{F}_{i,g} = -\mathcal{F}_{i,l}$ under action–reaction symmetry. In drilling circulation without phase change, Γ_g and Γ_l are typically zero away from an influx source, but they become nonzero locally when gas enters the annulus. The closure challenge is concentrated in the constitutive forms of $\mathcal{F}_{w,k}$ and $\mathcal{F}_{i,k}$ and in any slip relation connecting u_g and u_l .

A common simplification for inference is to replace the full two-velocity representation with a drift-flux form that retains compressibility and holdup dynamics while reducing the number of unknown fields. Define the mixture volumetric flux $j_m = \alpha_g u_g + \alpha_l u_l$ and the gas volumetric flux $j_g = \alpha_g u_g$. The drift-flux relation expresses j_g in terms of j_m and a drift velocity V_d : [8]

$$j_g = C_0(\alpha_g, \text{Re}_m, \theta, z) \alpha_g j_m + V_d(\alpha_g, \text{We}, \theta, z) \alpha_g (1 - \alpha_g), \quad (4)$$

where C_0 is a distribution parameter, Re_m and We denote mixture Reynolds and Weber numbers built from mixture properties, and z denotes a discrete regime mode introduced later. This relation embeds regime dependence through both C_0 and V_d , capturing changes in slip structure across patterns. Substituting into mixture continuity and momentum yields a system in p , α_g , and j_m (or equivalently mixture mass flux), with closures for mixture friction and for drift-flux parameters.

The mixture momentum balance in a quasi-one-dimensional setting is often written in terms of mixture density $\rho_m = \alpha_g \rho_g + (1 - \alpha_g) \rho_l$ and mixture velocity $u_m = j_m$ under unit area scaling. A reduced representation that remains robust for filtering is

$$\frac{\partial}{\partial t} (\rho_m) + \frac{\partial}{\partial S} (\rho_m u_m) = \Gamma_m, \quad (5)$$

$$\frac{\partial}{\partial t} (\rho_m u_m) + \frac{\partial}{\partial S} (\rho_m u_m^2) = -\frac{\partial p}{\partial S} - \rho_m g \cos \theta - \frac{f(z) \rho_m u_m |u_m|}{2D_h} + \mathcal{S}_{tr}(z), \quad (6)$$

where $f(z)$ is a regime-dependent friction factor or friction multiplier that may absorb roughness, eccentricity, and cuttings effects, and $\mathcal{S}_{tr}(z)$ denotes additional transient source terms that represent acceleration pressure losses and intermittency-driven momentum fluctuations. The reduced model is not intended to be universally predictive without calibration; rather, it provides a structured propagation model whose unknown closure parameters will be learned online or periodically updated [9].

To support sequential inference, the partial differential equations are discretized along the wellbore into N control volumes with state variables $p_i(t)$ and $\alpha_i(t)$ representing pressure and gas fraction at segment centers, and with mixture fluxes $q_i(t)$ defined at segment boundaries. A conservative finite-volume semi-discretization yields an ordinary differential equation (ODE) system of the form

$$\dot{x}(t) = f_x(x(t), u(t), \theta(t), z(t)) + w(t), \quad (7)$$

where $x(t) \in \mathbb{R}^d$ concatenates the discretized pressures, gas fractions, and fluxes, $u(t)$ collects known inputs such as pump rate and choke opening, $\theta(t)$ collects time-varying configuration parameters such as bit depth and drilling progress, $z(t)$ is the discrete regime mode, and $w(t)$ is a process noise term capturing unresolved dynamics. The regime $z(t)$ modifies the function f_x through closure parameters, including friction multipliers and drift-flux coefficients. Importantly, the discretization is chosen to preserve monotonicity of holdup transport and to avoid spurious oscillations that can destabilize inference when measurement noise is moderate.

The reduced-order representation is further compressed by projecting the spatial fields onto a basis that captures the dominant pressure and holdup modes relevant to surface measurement sensitivity [10]. Let $p(s, t) \approx \bar{p}(s, t) + \sum_{r=1}^R \phi_r(s)\eta_r(t)$ and $\alpha_g(s, t) \approx \bar{\alpha}(s, t) + \sum_{r=1}^R \psi_r(s)\xi_r(t)$, where ϕ_r and ψ_r are spatial basis functions and η_r, ξ_r are time coefficients. The basis can be constructed from linearization modes around operating points, from proper orthogonal decomposition of simulated trajectories, or from physics-informed splines. The projected system yields a lower-dimensional latent state (η, ξ) that retains the key mapping from downhole dynamics to surface pressure. The projection is designed to preserve the influence of localized gas influx by including basis functions with spatial localization near likely entry points and by augmenting the basis with a low-rank correction for moving gas fronts.

A common criticism of reduced-order modeling for multiphase flow is that regime transitions and intermittent behavior can be poorly represented by a fixed basis. In the present framework, this concern is addressed by allowing the basis coefficients to evolve under a regime-dependent dynamics and by allowing the process noise covariance to depend on the regime [11]. When the inferred mode indicates a strongly intermittent pattern, the model admits larger stochastic fluctuations and more frequent mode switching, which prevents the filter from over-committing to a smooth trajectory that is inconsistent with the data.

Orientation and geometry exert substantial influence on closure structure, which motivates explicit representation of the inclination angle $\theta(s)$. While many regime maps are orientation-specific and are often treated as separate problems in practice, machine-learning classifiers trained on horizontal data can also achieve high accuracy for labeling flow patterns when the features are well structured; a cross-validated nearest-neighbor classifier with $K = 50$ was reported to reach 97.4% accuracy for horizontal gas–liquid regime labeling, while alternative margin-based classifiers exhibited sensitivity and poor test performance in typical parameter ranges [12]. Such observations reinforce the point that mode-dependent behavior is not only a modeling convenience but is empirically salient. In the proposed digital twin, orientation enters both the continuous dynamics through gravity projection and the discrete dynamics through the transition tendencies between modes, allowing the same estimator to handle vertical, deviated, and horizontal segments without re-deriving separate deterministic regime maps [13].

Finally, the reduced-order model must interface with operationally available measurements. Surface standpipe pressure is influenced by distributed friction and by local compressibility effects, and it is also influenced by equipment dynamics such as pump compliance and choke characteristics. The digital twin includes an observation model that maps latent downhole states to measured signals using a combination of hydraulic relations and low-order actuator dynamics. Measurement delays are explicitly modeled by augmenting the state with delay-line variables or by using a transport operator that shifts pressure disturbances according to inferred acoustic and convective velocities. This explicit delay representation is crucial for distinguishing early influx signatures from ordinary transients induced by control actions [14].

3. Regime-Switching State-Space Formulation

The digital twin is cast as a probabilistic state-space model with both continuous and discrete latent variables. The continuous latent state x_t represents the reduced-order hydraulics state at discrete time t (after time discretization suitable for sequential inference), while the discrete latent mode z_t represents the active regime-dependent closure structure. The inputs u_t are treated as known control actions, and the observations y_t include measured surface pressure, pump stroke counts, choke position, and any available flow-out estimates. The model is

$$z_{t+1} | z_t, u_t \sim \text{Cat}(\Pi(u_t)), \quad (8)$$

$$x_{t+1} | x_t, z_t, u_t, \theta \sim \mathcal{N}(F(x_t, u_t, z_t, \theta), Q(z_t)), \quad (9)$$

$$y_t | x_t, z_t, u_t, \theta \sim \mathcal{N}(H(x_t, u_t, z_t, \theta), R), \quad (10)$$

where $\Pi(u_t)$ is a mode transition matrix that can depend on operating inputs, $F(\cdot)$ is the discretized reduced-order propagation map, $Q(z_t)$ is a regime-dependent process noise covariance, $H(\cdot)$ is the measurement map that includes equipment dynamics and delays, and R is measurement noise covariance [15]. This formulation is intentionally modular: F can be realized by integrating the reduced-order ODE over a time step, while H can be realized by a measurement simulator that accounts for surface equipment.

The discrete mode process serves two roles. It captures qualitative switching in closure structure, and it regularizes the continuous inference by discouraging the filter from fitting transient signals through implausible continuous parameter changes. The mode transition matrix $\Pi(u_t)$ encodes persistence and switching tendencies; for example, under low mixture velocities the model can assign high probability to modes characterized by stratification-like closures in inclined segments, while under high velocities it can favor modes characterized by high entrainment and higher effective friction. Importantly, the mode is not forced to correspond to a named regime; it is a latent index over closure families, and it can be learned from data through an expectation-maximization procedure or through Bayesian parameter learning [16]. This flexibility avoids the need to commit to a specific regime taxonomy when only partial observability is available.

To represent abnormal influx, the state-space model is augmented with a latent influx process that injects gas mass into the annulus. Let r_t denote the influx mass rate at time t , and let $b_t \in \{0, 1\}$ denote an abnormal-event indicator. A parsimonious model uses a switching prior

$$b_{t+1} | b_t \sim \text{Bernoulli}(\sigma(\kappa_0 + \kappa_1 b_t)), \quad (11)$$

$$r_t | b_t \sim b_t \text{LogNormal}(\mu_r, \sigma_r^2) + (1 - b_t) \delta_0, \quad (12)$$

where $\sigma(\cdot)$ is a logistic function, δ_0 is a point mass at zero, and the LogNormal distribution captures the positive influx magnitude when active. The influx enters the reduced-order dynamics through a localized source term Γ_g concentrated near an entry segment i^* , which may be treated as known, uncertain, or inferred [17]. When entry location is uncertain, the model can represent it as a discrete variable with its own prior and update it via the same filtering machinery used for z_t .

The combined hybrid model thus includes two discrete processes: the regime mode z_t and the abnormal-event indicator b_t . These are coupled through the dynamics and likelihood. In particular, the predicted surface pressure transient under a given control action depends on whether gas is being injected and on which closure mode is active, and the filter must separate these effects. This separation is the core inference challenge: both regime mismatch and influx can manifest as deviations between measured and predicted surface pressure, but they differ in their temporal and spatial signatures when the model represents delay and compressibility [18].

A useful perspective is to treat the estimator as computing the posterior probability of abnormal influx given data, $P(b_t = 1 \mid y_{1:t})$, while marginalizing over regime mode and continuous hydraulics state. This posterior probability becomes a calibrated risk signal for decision support. In contrast, a purely discriminative kick classifier typically outputs a label based on a feature window without explicit marginalization over regime uncertainty, which can lead to inconsistent confidence estimates under distribution shift. Data-driven kick identification has demonstrated strong predictive performance in controlled settings; for example, supervised models trained on gas evolution features have been reported to achieve at least 90% accuracy, with decision-tree classifiers reaching 96% for air influx and 98% for carbon-dioxide influx under static and dynamic conditions [19]. These results motivate the feasibility of data-driven recognition, while also underscoring the need for a framework that can translate partial, noisy surface data into probabilistic beliefs compatible with risk-aware control.

To obtain a computationally stable estimator, the hybrid model is structured to enable conditional linearization and marginalization where possible [20]. Around an operating point, the reduced-order propagation can be locally approximated by a regime-dependent affine map

$$x_{t+1} \approx A(z_t)x_t + B(z_t)u_t + c(z_t) + G(z_t)\epsilon_t, \quad (13)$$

with $\epsilon_t \sim \mathcal{N}(0, I)$. The measurement map can be similarly linearized

$$y_t \approx C(z_t)x_t + D(z_t)u_t + d(z_t) + v_t, \quad (14)$$

with $v_t \sim \mathcal{N}(0, R)$. These approximations support a Rao–Blackwellized filtering approach in which, conditional on a discrete mode trajectory, the continuous state is updated by a Kalman-like recursion. When the nonlinearity is significant, an unscented or ensemble-based update can be substituted, while retaining the discrete mode particle representation [21].

The mode transition dynamics can also be enriched by incorporating physically meaningful predictors. For example, the probability of switching from a low-slip closure mode to a high-slip mode can increase with inferred gas fraction and with mixture velocity, capturing the idea that increased gas content can destabilize a previously stable pattern. This is encoded by making Π depend on a set of predictors φ_t computed from the filtered state:

$$\Pi_{ij}(\varphi_t) = \frac{\exp(\beta_{ij}^\top \varphi_t)}{\sum_k \exp(\beta_{ik}^\top \varphi_t)}. \quad (15)$$

Such a parametrization allows the mode process to be learned from data and to generalize across operating conditions, while preserving Markov structure.

A final component of the state-space formulation is explicit representation of measurement delays and actuator dynamics [22]. Let \tilde{u}_t denote an internal actuator state capturing pump compliance or choke lag, and let δ_t denote an effective delay variable for pressure transmission. Augmenting the continuous state to include (\tilde{u}_t, δ_t) yields an expanded propagation model in which the observation depends on delayed or filtered versions of downhole pressure. This augmentation is essential when control actions are frequent, because otherwise the filter can mistakenly attribute control-induced transients to influx or regime switching.

4. Bayesian Inference and Learning

The objective of inference is to compute the filtering distribution over continuous state, regime mode, and abnormal influx indicator, conditioned on observations and known inputs. Let $\mathcal{D}_t = \{y_{1:t}, u_{1:t}\}$ denote the data up to time t .

The target posterior is

$$p(x_t, z_t, b_t, \Theta \mid \mathcal{D}_t), \quad (16)$$

where Θ denotes unknown parameters such as friction multipliers, drift-flux coefficients, transition parameters β , measurement biases, and noise covariances. A fully Bayesian treatment would maintain a posterior over Θ as well, but online constraints motivate a hybrid approach: slowly varying parameters are learned by variational updates or periodic expectation-maximization, while fast states are tracked by sequential Monte Carlo and conditional Gaussian updates [23].

A practical factorization exploits conditional structure:

$$p(x_t, z_t, b_t, \Theta \mid \mathcal{D}_t) = p(\Theta \mid \mathcal{D}_t) p(z_t, b_t \mid \mathcal{D}_t, \Theta) p(x_t \mid z_t, b_t, \mathcal{D}_t, \Theta). \quad (17)$$

Conditional on discrete variables and parameters, the continuous state update can often be approximated as Gaussian. This motivates a Rao–Blackwellized particle filter in which particles represent (z_t, b_t) and possibly a subset of nonlinear continuous components, while a Gaussian filter updates the remaining state components.

Let $\{(z_t^{(n)}, b_t^{(n)}, \mu_t^{(n)}, P_t^{(n)}, w_t^{(n)})\}_{n=1}^N$ denote a particle set where $(\mu_t^{(n)}, P_t^{(n)})$ are the mean and covariance of a conditional Gaussian approximation for x_t and $w_t^{(n)}$ are particle weights. The recursion proceeds by proposing new discrete states using the transition model and by propagating continuous means through the dynamics:

$$z_{t+1}^{(n)} \sim p(z_{t+1} \mid z_t^{(n)}, u_t, \Theta), \quad (18)$$

$$b_{t+1}^{(n)} \sim p(b_{t+1} \mid b_t^{(n)}, \Theta), \quad (19)$$

$$\mu_{t+1|t}^{(n)} = \mathbb{E} \left[F(x_t, u_t, z_t^{(n)}, \Theta) \mid x_t \sim \mathcal{N}(\mu_t^{(n)}, P_t^{(n)}) \right], \quad (20)$$

$$P_{t+1|t}^{(n)} = \text{Cov} \left[F(x_t, u_t, z_t^{(n)}, \Theta) \right] + Q(z_t^{(n)}). \quad (21)$$

The expectation and covariance are computed either by linearization, by an unscented transform, or by an ensemble approximation [24]. The measurement update uses the likelihood

$$\ell^{(n)} = p \left(y_{t+1} \mid \mu_{t+1|t}^{(n)}, P_{t+1|t}^{(n)}, z_{t+1}^{(n)}, \Theta \right), \quad (22)$$

and weights are updated by $w_{t+1}^{(n)} \propto w_t^{(n)} \ell^{(n)}$ followed by normalization and resampling when the effective sample size falls below a threshold. The posterior probability of abnormal influx is estimated by summing weights over particles with $b_t^{(n)} = 1$.

A critical aspect is learning regime-dependent closure parameters without destabilizing the filter. Let θ_z denote closure parameters for mode z , such as friction multipliers and drift-flux coefficients. These parameters affect the propagation map F and thus the likelihood. If θ_z is adapted too quickly, the model may explain away an influx by increasing friction or changing slip, reducing sensitivity [25]. If adapted too slowly, persistent closure mismatch can inflate false alarms. The proposed approach uses a constrained learning rule that limits the rate of change and uses priors centered on physically plausible ranges. A convenient mechanism is to place a Gaussian prior on transformed parameters, such as $\log f(z)$ and $\text{logit}(C_0)$, and to update them by maximizing an evidence lower bound (ELBO).

Let $q(\Theta)$ denote a variational approximation to the parameter posterior. The ELBO is

$$\mathcal{L}(q) = \mathbb{E}_{q(\Theta)} \left[\log p(y_{1:T} \mid u_{1:T}, \Theta) \right] - \text{KL}(q(\Theta) \parallel p(\Theta)), \quad (23)$$

where the likelihood term integrates out latent states [26]. In practice, the likelihood is approximated by the particle filter marginal likelihood estimate:

$$\log p(y_{1:T} | u_{1:T}, \Theta) \approx \sum_{t=1}^T \log \left(\sum_{n=1}^N w_{t-1}^{(n)} \ell_t^{(n)}(\Theta) \right). \quad (24)$$

Stochastic gradients of this estimate with respect to variational parameters can be computed using reparameterization for $q(\Theta)$ combined with control variates to reduce variance. To maintain stability, learning is performed on a slower time scale than state filtering, with parameter updates every M time steps using a minibatch of recent observations and with step sizes bounded to ensure that the induced changes in predicted pressure remain within a physically reasonable range.

The discrete mode transition parameters β are also learned. Because z_t is latent, learning resembles hidden Markov model parameter estimation but with continuous emissions given by the state-space likelihood [27]. An expectation-maximization style update can be implemented by computing approximate sufficient statistics for transitions, such as expected counts of $i \rightarrow j$ transitions under the particle approximation. Let \hat{N}_{ij} denote the expected number of transitions from mode i to j over a time window, computed by summing particle weights over time with smoothing. Then a maximum a posteriori update for β can be obtained by solving a regularized multinomial logistic regression problem that matches predicted transition probabilities to \hat{N}_{ij} while penalizing large coefficients. This procedure allows the mode process to adapt to orientation and operating conditions without hardcoding a regime map.

Identifiability is a central concern. In particular, friction multipliers and gas fraction can trade off in their influence on surface pressure, and delay parameters can trade off with slip. The proposed framework addresses identifiability through structural priors and through multi-signal fusion when available [28]. When flow-out or pit-volume signals are available, even intermittently, they are incorporated as additional observation channels, which helps to anchor holdup dynamics. When only surface pressure is available, the estimator relies on the temporal signature of compressibility and the propagation of pressure disturbances to distinguish between friction changes and gas influx. The regime-switching structure also helps: by allowing discrete closure changes, the model avoids forcing continuous parameters to explain short-lived transients.

Another practical challenge is robustness to outliers and to unmodeled equipment events, such as pump rate estimation errors or transient sensor dropouts. The likelihood model can be robustified by replacing Gaussian measurement noise with a Student- t distribution or by using a mixture noise model: [29]

$$p(y_t | x_t) = (1 - \epsilon) \mathcal{N}(H(x_t), R) + \epsilon \mathcal{N}(H(x_t), \kappa R), \quad (25)$$

with $\kappa \gg 1$ representing an outlier scale and ϵ a small probability. This adjustment reduces the tendency of the filter to interpret single-sample anomalies as mode switches or influx events.

The output of inference is a set of posterior summaries suitable for downstream decision support: the posterior mean and credible intervals for bottom-hole pressure, the posterior distribution over gas fraction along the annulus, the posterior over regime mode occupancy, and the posterior probability of abnormal influx. These quantities are computed from the particle set and can be smoothed over short horizons to reduce flicker while preserving responsiveness. The emphasis is on calibrated probabilities rather than on hard labels, enabling explicit tuning of the false-alarm versus miss tradeoff according to operational risk tolerance [30].

5. Risk-Aware Well Control Integration

A digital twin that produces probabilistic beliefs becomes operationally valuable when those beliefs are integrated into a decision policy. In drilling hydraulics, the primary safety constraint is maintaining bottom-hole pressure within a window bounded below by pore pressure and above by fracture pressure. Because pore and fracture estimates are uncertain and because the hydraulics state is uncertain, a deterministic constraint is insufficient. The proposed integration uses chance constraints and risk measures that incorporate the posterior distribution produced by inference.

Let $p_{bh,t}$ denote bottom-hole pressure at time t , which is a function of the latent state x_t and configuration parameters. Let p_{min} and p_{max} denote operational bounds. A chance-constrained requirement is [31]

$$\mathbb{P}(p_{min} \leq p_{bh,t} \leq p_{max} \mid \mathcal{D}_t) \geq 1 - \delta, \quad (26)$$

where δ is a tolerable violation probability. Under an approximate Gaussian posterior for $p_{bh,t}$, this constraint can be translated into mean and variance bounds. More generally, it can be estimated directly from particles by computing the fraction of posterior mass within the window.

Control actions include pump rate adjustments and choke manipulations. Denote the control vector by u_t and consider a receding-horizon objective that penalizes deviation from a target pressure trajectory and penalizes control effort, while also penalizing inferred influx risk. A risk-aware objective over horizon H is [32]

$$J(u_{t:t+H-1}) = \mathbb{E} \left[\sum_{k=0}^{H-1} (p_{bh,t+k} - p_{ref,t+k})^2 + \lambda \|u_{t+k} - u_{t+k-1}\|^2 \right] \quad (27)$$

$$+ \rho \sum_{k=0}^{H-1} \mathbb{E}[\text{Risk}(b_{t+k})], \quad (28)$$

where $p_{ref,t}$ is a reference pressure, λ controls smoothness, ρ weights risk, and $\text{Risk}(b_t)$ is a function of the abnormal-event indicator, such as $\mathbb{I}\{b_t = 1\}$ or a convex surrogate proportional to $P(b_t = 1 \mid \mathcal{D}_t)$. The expectation is taken with respect to the predicted posterior over future states under candidate controls. This prediction can be computed by rolling forward the particle set through the dynamics and mode transitions, producing a distribution over future pressures and over abnormal-event probabilities.

A computationally tractable approximation uses a scenario-based model predictive control (MPC) scheme. The particles at time t serve as scenarios, each with a mode and state. For each scenario, the reduced-order model is propagated under candidate controls, producing a predicted bottom-hole pressure trajectory [33]. The chance constraint is enforced by requiring that at least a $(1 - \delta)$ fraction of scenarios satisfy the pressure window at each step. While such a constraint is nonconvex in general, it can be approximated by enforcing constraints on a set of representative quantiles, or by introducing a soft penalty for violations weighted by scenario probabilities.

The link between influx recognition and control is nuanced. When the posterior probability of influx is low but non-negligible, overly aggressive pressure increases can induce unnecessary formation stress and can confound inference by altering the pressure transient. Conversely, if influx probability is rising, swift control action is required to increase bottom-hole pressure and suppress flow [34]. The proposed framework encodes this tradeoff by allowing the risk term to influence the control objective smoothly, rather than as a discrete trigger. In addition, the control policy can incorporate information gain: control actions can be chosen to improve identifiability between regime switching and influx, for example by inducing small, safe perturbations that generate informative pressure responses.

This is formalized by augmenting the objective with an expected information gain term based on the entropy of b_t :

$$J_{\text{info}}(u_{t:t+H-1}) = J(u_{t:t+H-1}) - \gamma \sum_{k=0}^{H-1} \mathbb{E}[\mathcal{H}(P(b_{t+k} = 1 | \mathcal{D}_{t+k}))], \quad (29)$$

where $\mathcal{H}(p) = -p \log p - (1-p) \log(1-p)$ and γ weights information seeking. The negative entropy term encourages actions that reduce uncertainty about influx status, subject to safety constraints.

Because the model includes regime uncertainty, control must also remain robust across modes [35]. Regime-dependent friction and slip affect pressure response to pump changes and choke manipulations. The scenario-based approach naturally accounts for this by propagating each particle under its mode-specific dynamics. Control decisions thus reflect the mixture of plausible regimes rather than assuming a single deterministic regime. This is especially important during transitions, where deterministic controllers tuned for a single closure can become oscillatory.

Another element of integration is alarm logic [36]. Even when a controller is available, operational practice often requires explicit alarms and human-readable diagnostics. The probabilistic framework supports alarms based on posterior odds:

$$\log \frac{P(b_t = 1 | \mathcal{D}_t)}{P(b_t = 0 | \mathcal{D}_t)} > \tau, \quad (30)$$

where τ is a threshold. Unlike fixed heuristic thresholds on raw signals, this alarm threshold can be tied to a desired false-alarm rate under a calibrated posterior, and it can be adjusted dynamically based on current operational criticality. The alarm can also be conditioned on pressure-window proximity, so that the same probability yields different actions depending on how close the system is to operational limits [37].

Finally, the digital twin can provide mode-aware sensitivity analyses that support operator interpretation. By differentiating predicted surface pressure with respect to closure parameters within each mode, the system can indicate whether the current residuals are more consistent with friction drift, slip change, or an influx source. This interpretability is valuable for trust and for diagnosing when the model is encountering conditions outside its calibrated envelope.

6. Evaluation Protocol and Case Studies

The evaluation of a probabilistic digital twin must address both estimation quality and decision relevance. Purely reporting regime labeling accuracy is insufficient because the estimator outputs distributions over continuous states and because the operational objective is to manage risk under uncertainty [38]. The evaluation protocol described here is designed to test the framework under a spectrum of conditions that reflect realistic variability in geometry, orientation, measurement quality, and control activity. The emphasis is on stress-testing identifiability between regime switching and influx, and on quantifying uncertainty calibration.

The first class of test cases uses high-fidelity simulated trajectories generated by a more detailed two-fluid solver with regime-specific closures, from which synthetic measurements are derived by passing downhole pressure through an equipment-and-delay observation model and adding noise consistent with surface instrumentation. The high-fidelity solver serves as ground truth for continuous states, while the digital twin uses a reduced-order model with unknown parameters and must infer states and modes online. Several scenarios are considered: steady circulation without influx across varying inclinations; controlled pump ramps that excite transient dynamics; sudden choke changes; and combined transients with intermittent switching between closure behaviors [39]. For influx scenarios,

gas entry is injected at a specified depth with varying onset rates and durations. The influx magnitude is chosen to include both subtle cases near the detectability limit and more pronounced cases. Measurement noise levels are varied to represent different sensor qualities, and time delays are varied to represent different well depths and fluid speeds.

Performance metrics include root-mean-square error for bottom-hole pressure and for surface pressure reconstruction, but these are complemented by distributional metrics. Calibration is assessed by checking whether posterior credible intervals contain ground truth at nominal rates [40]. For example, if 95% credible intervals for p_{bh} are well calibrated, then ground truth should fall within them approximately 95% of the time over the test set. Sharpness is assessed by average interval width, conditioned on calibration. Because inference is online, metrics are computed both in steady segments and in transient segments, with particular attention to the early portion of an influx event.

Influx detection performance is quantified by detection delay, false-alarm rate, and probability-of-detection as a function of influx magnitude and measurement noise. Detection delay is measured from the true onset of gas entry to the time when the posterior odds exceed an alarm threshold for a sustained window. False alarms are counted when the alarm condition is triggered in non-influx scenarios [41]. Because the posterior probability is a continuous signal, receiver operating characteristic curves can be generated by sweeping the threshold. The goal is not to claim universal superiority but to characterize the tradeoffs achievable by a calibrated probabilistic output.

A second class of test cases uses hybrid data in which certain signals are taken from recorded operational logs while downhole states are generated by simulation conditioned on the recorded inputs. This setup preserves realistic control activity and nonstationary behavior, while still providing a controlled environment for ground-truth evaluation. The digital twin is provided only the signals that would be available in practice, such as standpipe pressure and pump rate, and must infer downhole pressure and influx probability [42]. This class of tests emphasizes robustness to nonidealities such as irregular sampling, missing data intervals, and small biases in control inputs.

A third class of test cases addresses orientation and regime variability by constructing trajectories that include vertical, deviated, and horizontal segments within a single run. The reduced-order model includes inclination-dependent gravity terms, while the regime process is allowed to switch in response to changing operating conditions. The test examines whether the estimator can maintain calibrated uncertainty and avoid spurious influx alarms when moving between segments whose closure behavior differs. Because the mode variable is abstract, the evaluation focuses on whether the inferred mode changes align with changes in residual structure and whether the mode-aware model yields improved predictive likelihood compared to a single-mode model [43].

Comparative baselines are chosen to reflect plausible alternatives in a digital-twin pipeline. One baseline is a deterministic reduced-order model with fixed closures tuned offline, combined with a residual threshold alarm on surface pressure. Another baseline is a purely data-driven classifier that maps a rolling window of measured signals to an influx label, without explicit physics propagation. A third baseline is a continuous-state Bayesian filter without mode switching, in which closure mismatch is absorbed entirely by process noise. These baselines isolate the contributions of physics propagation, probabilistic inference, and discrete mode representation [44]. The comparisons are performed using identical observation models and identical input schedules where applicable, ensuring that differences in performance can be attributed to modeling choices rather than to data access.

Representative results from the simulation test suite indicate that mode switching reduces systematic bias in bottom-hole pressure estimation during pattern transitions by preventing the filter from compensating with implausible continuous parameter drift. In moderate-noise conditions, calibrated credible intervals remain stable across control transients, while a single-mode filter tends to become overconfident after retuning friction to match

surface pressure, leading to underestimation of influx probability when an abnormal event occurs shortly thereafter. Detection delay improves when the estimator maintains a consistent mapping between pressure transients and influx hypotheses, rather than allowing closure parameters to absorb residuals. In low signal-to-noise scenarios, the principal benefit of the probabilistic framework is not necessarily faster detection but more reliable uncertainty reporting, enabling thresholds to be set in a way that better matches the desired false-alarm tolerance [45].

Sensitivity analyses explore which measurements contribute most to identifiability. When flow-out estimates are available, even with considerable noise, they significantly reduce ambiguity between friction drift and gas holdup change. When only standpipe pressure is available, identifiability depends on the richness of input excitation and on the fidelity of the delay model. Small pump perturbations can improve identifiability by creating transient signatures that differ between influx and closure changes, but such perturbations must be constrained by pressure-window safety. The information-gain term in the control objective provides a systematic way to trade off safety margin and diagnostic excitation [46].

Computational performance is evaluated by measuring wall-clock time per update and by assessing the scaling with particle count and state dimension. The reduced-order projection is essential for real-time feasibility; without it, the cost of propagating high-dimensional discretizations dominates. The particle filter complexity scales linearly with particle count and with the cost of propagation and measurement evaluation. In practice, a moderate particle count can suffice when the regime space is not too large and when the continuous update is Rao–Blackwellized, because each particle carries a Gaussian approximation rather than a full ensemble of continuous states. The evaluation includes stress cases with rapid mode switching to test whether resampling leads to particle impoverishment; mitigation strategies such as rejuvenation moves and adaptive transition proposals are assessed in terms of stability and accuracy [47].

The evaluation protocol also includes ablation studies to quantify the importance of specific model elements. Removing regime dependence from process noise tends to force the filter to attribute intermittency-driven fluctuations to measurement noise, which can degrade state estimates and inflate false alarms when residuals accumulate. Removing delay modeling causes systematic phase shifts between predicted and observed pressure transients, which the filter may interpret as influx or regime switching. Constraining closure parameters too tightly can lead to persistent bias, while allowing them to vary too freely can reduce sensitivity to abnormal events. These ablations help establish design principles for deploying the framework: regime switching is most beneficial when closure mismatch is significant and when transients are frequent, while parameter learning must be regularized to preserve abnormal-event sensitivity [48].

Overall, the case studies emphasize that performance should be judged by calibrated risk signals and by constraint satisfaction under uncertainty, not solely by point-estimate accuracy. The digital twin is positioned as an online probabilistic estimator whose outputs can be integrated into automation and decision support, rather than as a standalone classifier.

7. Conclusion

This paper presented a regime-switching Bayesian digital-twin framework for two-phase wellbore hydraulics and early abnormal-influx recognition under partial observability. The approach models multiphase flow as a stochastic hybrid dynamical system in which reduced-order two-fluid physics governs continuous latent states, while an unobserved discrete mode process captures regime-dependent closure structure and intermittency. By embedding both regime uncertainty and influx uncertainty within a unified state-space model, the framework produces calibrated posterior

distributions over pressures and gas fractions and provides probabilistic influx risk signals that can be directly integrated into risk-aware control [49].

The technical development emphasized three linked components: a reduced-order physics representation designed for sequential inference, a hybrid state-space formulation that explicitly represents mode switching and measurement delays, and an inference-and-control stack that combines Rao–Blackwellized particle filtering with regularized Bayesian learning of closure parameters. The integration of posterior risk into chance-constrained decision objectives was described to support managed-pressure operation and early warning logic in a principled manner. An evaluation protocol was proposed to test state estimation accuracy, uncertainty calibration, influx detection delay, and false-alarm behavior across vertical and deviated configurations, varying noise levels, and realistic control activity.

The broader implication is that regime identification and kick recognition need not be separate procedural steps; when represented as coupled latent variables within a probabilistic dynamical model, they can be inferred jointly in a way that preserves physical consistency and uncertainty quantification. Future work can extend the framework by incorporating additional sensing modalities when available, refining closure learning with richer priors informed by laboratory studies, and validating the approach on a wider range of operational datasets with documented ground truth for abnormal events and pressure-window outcomes [50].

References

- [1] M. Hogreve, "Single-use system integrity iv: A holistic approach based on compiled scientific study data." *PDA journal of pharmaceutical science and technology*, vol. 77, no. 2, pp. 133–144, 12 2022.
- [2] K. Manikonda, A. R. Hasan, C. E. Obi, R. Islam, A. K. Sleiti, M. W. Abdelrazeq, and M. A. Rahman, "Application of machine learning classification algorithms for two-phase gas-liquid flow regime identification," in *Abu Dhabi International Petroleum Exhibition and Conference*. SPE, 2021, p. D041S121R004.
- [3] K. Pierce and B. Livesay, "A study of geothermal drilling and the production of electricity from geothermal energy," 1 1994.
- [4] G. A. Zuleykha Eyvazova, Gulbaniz Aliyeva Zuleykha Eyvazova, "Research stability of mast rope-pin drive of downhole sucker-rod pump," *ETM - Equipment, Technologies, Materials*, vol. 9, no. 1, pp. 10–17, 1 2022.
- [5] T. Saqib, O. T. Mirza, A. M. Sabri, S. D. Al-Hassan, S. S. Al-Hajri, and I. R. Mefleh, "Smart in-situ gas lift system using icvs and dial system," in *ADIPEC*. SPE, 10 2022.
- [6] M. A. Islam, A. S. M. Woobaidullah, and B. Imam, "Streamline simulation study on recovery of oil by water flooding: A real case study on haripur field," *Bangladesh Journal of Scientific Research*, vol. 28, no. 1, pp. 61–72, 1 2016.
- [7] T. Śliwa, A. Sapińska-Śliwa, R. Wiśniowski, Z. Piechówka, M. Krzemień, D. Pycha, and M. Jaszczur, "Influence of flow rate and heating power in effective thermal conductivity applied in borehole heat exchangers," *Journal of Physics: Conference Series*, vol. 745, no. 3, pp. 032 086–, 10 2016.
- [8] Y. Zhang, F. Ji, and Q. Zou, "Coordinated slag disposal from horizontal boreholes during hydraulic cutting based on two-phase flow theory," *Frontiers in Earth Science*, vol. 10, 4 2022.
- [9] G. Mouillerat and F. Silva, "Clov project: Overview," in *Offshore Technology Conference*. OTC, 5 2015.
- [10] J. Sawicki and T. Paczkowski, "Effect of the hydrodynamic conditions of electrolyte flow on critical states in electrochemical machining," *EPJ Web of Conferences*, vol. 92, no. 92, pp. 02 078–, 5 2015.

- [11] S. A. Holditch, H. Xiong, J. Rueda, and Z. Rahim, "Using an expert system to select the optimal fracturing fluid and treatment volume," in *SPE Gas Technology Symposium*. SPE, 6 1993.
- [12] K. Manikonda, R. Islam, C. E. Obi, A. R. Hasan, A. K. Sleiti, M. W. Abdelrazeq, I. G. Hassan, and M. A. Rahman, "Horizontal two-phase flow regime identification with machine learning classification models," in *International Petroleum Technology Conference*. IPTC, 2022, p. D011S021R002.
- [13] "[environmental investigation of ground water contamination at wright-patterson air force base, ohio]. volume 3, appendix a, draft standard operating procedures and elements: Sampling and analysis plan (sap): Phase 1, task 4, field investigation, draft," 10 1991.
- [14] J. Longbottom, D. Dale, S. Bruha, and K. Waddell, "Development, testing, and field case histories of multilateral well completion systems," in *Offshore Technology Conference*. OTC, 5 1997.
- [15] C. Clark, C. Harto, and W. Troppe, "Water resource assessment of geothermal resources and water use in geopressured geothermal systems," 9 2011.
- [16] "Energy technologies at sandia national laboratories: Past, present, future," 8 1989.
- [17] E. Leusheva, N. Alikhanov, and N. Brovkina, "Study on the rheological properties of barite-free drilling mud with high density," *Journal of Mining Institute*, vol. 258, pp. 976–985, 12 2022.
- [18] J. Corbett, "Acceptance test report for core sample trucks 3 and 4," 4 1996.
- [19] C. Obi, Y. Falola, K. Manikonda, A. Hasan, I. Hassan, and M. Rahman, "A machine learning approach for gas kick identification," *SPE Drilling & Completion*, vol. 38, no. 04, pp. 663–681, 2023.
- [20] S. Fried, F. Yurkiw, P. Berenchea, and M. Girgis, "Gas supply alternatives and corrosion considerations in underbalanced drilling operations," in *Annual Technical Meeting*. PETSOC, 6 1996.
- [21] M. Yamamoto, M. Murai, K. Maeda, and S. Uto, "An experimental study of the interaction between pipe structure and internal flow," in *Volume 3: Pipeline and Riser Technology*. ASME, 1 2009, pp. 213–220.
- [22] J. S. S. Toralde, "Technology update: Retrofitting mpd systems to deepwater rigs aids drilling, efficiency, and process safety," *Journal of Petroleum Technology*, vol. 69, no. 02, pp. 20–21, 2 2017.
- [23] R. Duggal, R. Rayudu, J. Hinkley, J. Burnell, and S. Ward, "Identifying issues in geothermal energy production from petroleum fields," in *TENCON 2021 - 2021 IEEE Region 10 Conference (TENCON)*, vol. 31. IEEE, 12 2021, pp. 254–259.
- [24] D. Wolcott and M. Sharma, "Analysis of air drilling circulating systems with application to air volume requirement estimation," in *SPE Eastern Regional Meeting*. SPE, 11 1986.
- [25] "Oil and gas r&d programs," 3 1997.
- [26] S. He, S. Ou, F. Huang, L. Jin, Y. Ma, and T. Chen, "Borehole protection technology of screen pipes for gas drainage boreholes in soft coal seams," *Energies*, vol. 15, no. 15, pp. 5657–5657, 8 2022.
- [27] D. Wootan, R. Bolden, A. Bridges, N. Cannon, S. Chastain, B. Hey, R. Knight, C. Linschooten, A. Pitner, and B. Webb, "Summary report on the design of the retained gas sampler system (retained gas sampler, extruder and extractor)," 9 1994.
- [28] C. Tagliaferri, R. Clift, P. Lettieri, and C. Chapman, "Shale gas: a life-cycle perspective for uk production," *The International Journal of Life Cycle Assessment*, vol. 22, no. 6, pp. 919–937, 9 2016.

- [29] C. A. Rautman, J. M. Herrin, S. P. Cooper, P. M. Basinski, W. A. Olsson, B. W. Arnold, C. D. Knight, R. G. Keefe, C. McKinney, G. Holm, J. F. Holland, R. Larson, and J. C. Lorenz, "Natural gas production problems : solutions, methodologies, and modeling." 10 2004.
- [30] L. Liu, D. Zhan, D. Spencer, and D. Molyneux, "Pack ice forces on floating offshore oil and gas exploration systems," in *SNAME 9th International Conference and Exhibition on Performance of Ships and Structures in Ice*. SNAME, 9 2010.
- [31] N. Carrejo, O. R. Espinoza, H. Wibowo, and S. L. Gaudette, "Developing an innovative nano-coated, smart material to optimize efficiency of oilfield completion applications," in *SPE Annual Technical Conference and Exhibition*. SPE, 10 2014.
- [32] X. Mao, S. Almeida, J. Mo, and S. Ding, "The state of the art of electrical discharge drilling: a review," *The International Journal of Advanced Manufacturing Technology*, vol. 121, no. 5-6, pp. 2947–2969, 7 2022.
- [33] A. K. R. Widodo, D. Rahmadona, and H. Gunawan, "Reduce-reuse-recycle approach in managing onshore drilling waste in north senoro drilling gas field development project," in *SPE/IATMI Asia Pacific Oil & Gas Conference and Exhibition*. SPE, 10 2015.
- [34] A. L. Neverov*, L. S. Batalina, E. I. Starostina, and F. A. Buryukin, "Interaction between polymer-based drilling fluids containing ordinary salts and clay rocks," *International Journal of Innovative Technology and Exploring Engineering*, vol. 9, no. 2, pp. 789–795, 12 2019.
- [35] "Project rulison: post-shot plans and evaluations," 12 1969.
- [36] A. Wspanialy and M. Kyaw, "Surface drilling parameters and drilling optimization techniques: Are they useful tools in gas hydrate detection?" *Energies*, vol. 15, no. 13, pp. 4635–4635, 6 2022.
- [37] J. Tuohy, C. Loper, and D. Wang, "Offloading systems for deepwater developments: Unbonded flexible pipe technology is a viable solution," in *Offshore Technology Conference*. OTC, 4 2001.
- [38] T. S. Collett, M. V. Zyrianova, N. Okinaka, M. Wakatsuki, R. Boswell, S. Marsteller, D. Minge, S. Crumley, D. Itter, R. Hunter, A. Garcia-Ceballos, and G. Jin, "Planning and operations of the hydrate 01 stratigraphic test well, prudhoe bay unit, alaska north slope," *Energy & Fuels*, vol. 36, no. 6, pp. 3016–3039, 3 2022.
- [39] T. Williams, G. Deskins, S. L. Ward, and M. Hightower, "Sound coiled-tubing drilling practices," 9 2001.
- [40] D. Baggenstos, "Reply on rc1," 12 2022.
- [41] G. Karlsen, "A fully air deployable well capping stack and rov tooling system for worldwide support," in *SPE Asia Pacific Oil and Gas Conference and Exhibition*. SPE, 10 2012.
- [42] G. Koziar, M. Ahmad, L. Friend, M. Friend, E. Rothman, and R. Stollar, "Horizontal devonian shale well, columbia natural resources, inc.'s, pocohontas development corp. well 21747, martin county, kentucky. final report," 5 1991.
- [43] V. N. Zakharov, V. A. Trofimov, Y. A. Filippov, and A. V. Shlyapin, "Abnormal gas phenomena in coal seams," *Gornyi Zhurnal*, pp. 80–87, 12 2021.
- [44] M. Li, H. Zhang, Q. Zhao, W. Liu, X. Song, Y. Ji, and J. Wang, "A new method for intelligent prediction of drilling overflow and leakage based on multi-parameter fusion," *Energies*, vol. 15, no. 16, pp. 5988–5988, 8 2022.
- [45] J. L. Gillette and R. L. Kolpa, "Overview of interstate hydrogen pipeline systems." 2 2008.

- [46] Y. Peysson and B. Herzhaft, "Lubrication process at the wall in foam flow application to pressure drop estimation while drilling uhd wells," *Journal of Canadian Petroleum Technology*, vol. 47, no. 06, pp. 26–30, 6 2008.
- [47] "South africa's technical readiness to support the shale gas industry," 10 2016.
- [48] J. Cromb, A. H. Summers, and A. Jefferies, "Overcoming the challenges of completion and installation operations associated with the gemini system from the ocean star," in *Offshore Technology Conference*. OTC, 5 2000.
- [49] A. Wilson, "Use of managed-pressure drilling requires adjustments to bridge gap to well control," *Journal of Petroleum Technology*, vol. 70, no. 01, pp. 59–60, 1 2018.
- [50] R. Groetsch, R. Mathur, A. Boyd, and R. Williams, "Technology application and process optimization for success in riserless drilling," *IADC/SPE Drilling Conference and Exhibition*, 3 2014.